

# EVALUATION OF A HYBRID BIOCOMPOSITE OF HA/HDPE REINFORCED WITH MULTI-WALLED CARBON NANOTUBES (MWCNTs) AS A BONE-SUBSTITUTE MATERIAL

## OVREDNOTENJE HIBRIDNEGA BIOKOMPOZITA HA/HDPE OJAČANEGA Z VEČ-STENSKIMI OGLJIKOVIMI NANOCEVČICAMI (MWCNT), UPORABNEGA KOT KOSTNI NADOMESTEK

Ali A. Al-allaq<sup>1,2\*</sup>, Jenan S. Kashan<sup>3</sup>, Mohamed T. El-Wakad<sup>4</sup>,  
Ahmed M. Soliman<sup>2</sup>

<sup>1</sup>Ministry of Higher Education and Scientific Research, Office for Reconstruction and Projects, Baghdad, Iraq

<sup>2</sup>Biomedical Engineering Department, Faculty of Engineering, Helwan University Cairo, Egypt

<sup>3</sup>Biomedical Engineering Department, University of Technology, Baghdad, Iraq

<sup>4</sup>Faculty of Engineering and Technology, Future University, Cairo, Egypt

*Prejem rokopisa – received: 2021-05-20; sprejem za objavo – accepted for publication: 2021-07-12*

doi:10.17222/mit.2021.162

In this investigation, multi-wall carbon nanotubes (MWCNTs) with various percentages including 0.6, 1, 1.4 and 2 % were combined into high-density polyethylene (HDPE 60 w%) and hydroxyapatite (HA 40 w%) to form a biocomposite, using hot-press techniques. The surface topography shown by AFM images illustrates the differences in the roughness of the samples' surfaces with different percentages of added MWCNTs. The DSC technique exhibits the effect of adding MWCNTs in different percentages, creating a degree of crystallinity that affects the mechanical properties of the samples. The *in vitro* bioactivity was investigated by immersing the samples in Ringer's solution acting as simulated body fluid (SBF) for (0, 3, 6, 9, 12) d. The FE-SEM and EDX image explained the HA layers formed on a sample's surface after 3 d in Ringer's solution. Based on the XRD technique, after being immersed in Ringer's solution, the HA crystallographic structure forms monetite. The enhancement of bioactivity was shown during the incorporation of MWCNTs into the HA/HDPE composite. These results exhibited excellent indications of biocompatibility properties with a possibility of making promising biomaterials for making bone-substitute applications.

Keywords: bone-tissue engineering, biomaterials, bone scaffold

V pričujočem članku avtorji opisujejo izdelavo biokompozita s tehniko vročega stiskanja. Kompozit je bil izdelan z matrico iz 60 w% visoko gostega polietilena (HDPE) in 40 w% hidroksiapatita (HA;  $\text{Ca}_{10}(\text{PO}_4)_6(\text{OH})_2$ ). Kot ojačitvena faza je bila uporabljena različna vsebnost (0,6, 1, 1,4 in 2 w%) več-stenskih ogljikovih nano-cevčic (MWCNT). Slike površinske topografije kompozita dobljene s pomočjo mikroskopije na atomsko silo (AFM; Atom force Microscopy), kažejo razlike v hrapavosti površine glede na vsebnost dodanih MWCNT. Diferencialna vrstična kalorimetrija (DSC) je pokazala vpliv dodatka MWCNT na stopnjo kristaliničnosti kompozita, kar vpliva na njegove mehanske lastnosti. Avtorji članka so določevali bioaktivnost kompozita *in vitro* s postopkom potapljanja vzorcev za 3, 6, 9 in 12 dni v Ringerjevo raztopino, ki simulira telesno tekočino (SBF; angl.: simulated body fluid). S pomočjo vrstične elektronske mikroskopije (FE-SEM) in rentgenske energijske disperzijske spektroskopije (EDX) so pojasnili plasti HA, ki so nastale na površini vzorcev po tri dnevem zadrževanju vzorcev kompozita v Ringerjevi raztopini. Po potapljanju vzorcev v Ringerjevo raztopino so s pomočjo XRD tehnike ugotovili, da ima HA kristalografsko strukturo monetita. Z dodatkom MWCNT v HA/HDPE biokompozit se je povečala njegova bioaktivnost. To kaže na odlično biokompatibilnost tega kompozita in možnost njegove uporabe kot kostnega nadomestka.

Ključne besede: inženiring kostnih tkiv, biomateriali, kostni gradnik

## 1 INTRODUCTION

Bone is a specialized connective tissue, highly organized and complex. It is physically characterized as a hard, rigid and strong tissue; when investigated microscopically, its appearance consists of relatively few cells and a lot of intercellular material made of stiffening elements and collagen fibers. The best bone substitutes and grafts are naturally those with biological and biomechanical characteristics that match the normal bone.<sup>1</sup>

Bone grafting is one of the most frequently applied medical techniques for increasing bone regeneration in orthopaedics surgery. This method has many limitations and risks for the patient. So, the evolution of artificial bone and use of substitute materials that do not affect healthy tissue, causing bacterial or viral risk to the patients, and can be provided at any time, in any amount are preferred.<sup>2,3</sup> Calcium phosphate bioceramics, such as hydroxyapatite (HA) nanoparticles, have been largely used as synthetic bone-replacement materials for orthopaedics and dental treatments. HA has been the base mineral constituent of human bones and teeth because of its excellent bioactivity and biocompatibility.<sup>4,5</sup> Polyeth-

\*Corresponding author's e-mail:  
ali.martial85@gmail.com (Ali A. Al-allaq)

ylene is one type of biocompatible polymers. It has many features such as easy formability, inertness and excellent stability in body fluids. Due to its physical properties (modulus/strength), polyethylene can be used for load-bearing hard-tissue prosthesis applications. Many researchers attempted to improve hydroxyapatite's mechanical properties by using reinforcing materials to match the natural-bone specifications and investigating their bioactivity level.<sup>6</sup> Carbon nanotubes (CNTs) have large aspect ratios, extremely high surface areas and signally high mechanical strength. These extraordinary features make nanotubes good candidates as fillers in various ceramics and polymers used for achieving desired properties. It can be expected that combining polymeric materials with CNTs will modify the surface characteristics of CNTs. This combining can modify their toxicity without affecting their particular characteristics and potential for future applications.<sup>7</sup>

MWCNTs can increase the interfacial interaction between a polymer matrix and MWCNTs due to their chemical functionalization. This feature improves the adhesion of MWCNTs to polymers and various organic solvents. Also, it improves dispersion and reduces the tendency to agglomerate. The improved interactions between a polymer matrix and MWCNTs enhance the polymer's load transfer to the nanotubes and improve the reinforcement efficiency.<sup>8</sup>

Many investigations strived to improve hydroxyapatite's mechanical features by using reinforcing materials to match the natural-bone properties, and investigating their bioactivity level. Several studies attempted to apply CNTs as a new method of improving the mechanical properties of polyethene,<sup>9</sup> hydroxyapatite (HA)<sup>10</sup> and composites of HA/HDPE.<sup>11</sup> Numerous studies found that CNTs increase the proliferation and adhesion of osteoblasts and fibroblasts. However, the biocompatibility with these cells may depend on the surface energy and diameter of the CNTs. In other investigations, CNTs were also reported to decrease the proliferation and toxicity of osteoblast cells. So, the CNT reinforcement of

nanocomposites for bone implants still requires more investigation before it can be approved as a biocompatible material, especially with regard to bone-cell applications.<sup>10</sup> In order to examine the biological activity, many studies attempted to prove the effectiveness of certain biocomposites, providing suitable results regarding bone-substitute materials.<sup>12-14</sup> This work aims to investigate the effect of additions of various weight percentages (w/%) of MWCNTs to a hybrid (HA, HDPE) biocomposite on the bioactivity properties to form a biocomposite material that can be used as a bone substitute. Samples were fabricated using the hot-press technique. The *in vitro* investigation used Ringer's solution as simulated body fluid (SBF).

## 2 MATERIALS AND METHODS

### 2.1 Production of hybrid biocomposite samples

HDPE powder with a particle size of 5  $\mu\text{m}$  was purchased from Right Fortune Industrial Limited (Shanghai, China). MWCNTs with a purity of 90 % were provided from Cheap Tubes Inc., USA. HA nanoparticles with a particle size of 20 nm, a powder purity of approximately 99 % and a density of 3140  $\text{kg}/\text{m}^3$  were obtained from MK Nano (Toronto, Canada). The composition of HA/HDPE was 40 w/% HA/60 w/% HDPE, while the amounts of the MWCNT addition were (0.6, 1, 1.4 and 2) %. The hot-pressing technique used for composite shaping was employed to fabricate all the specimens. The pressure was applied hydraulically using Instron 1195, while heating was produced externally, using external heaters. The mold was heated to 150  $^{\circ}\text{C}$  and held at this temperature for 15 min. The melt-pressure value was 29 MPa for the samples molded. **Figure 1** shows a summary of the sample-fabrication process.

### 2.2 Atomic force microscopy (AFM)

An atomic force microscope (Ntegra NT-MDT, Russia) was used to investigate the surface topography (surface roughness and particles size). The resulting images were processed using the Nova<sup>TM</sup> software. The examination was performed under ambient conditions by applying the tapping mode.

### 2.3 Differential scanning calorimetry (DSC)

A DSC furnace is an isolated container provided with a heat flux plate with a thermopile and thermocouples measuring the heat flow to both the reference and sample containers. A differential scanning calorimeter (DSC-60, Shimadzu, Japan) was used. The sample mass (about 5 mg) was sealed in aluminum pans, then heated at a constant degree rate (5  $^{\circ}\text{C}/\text{min}$ ) in a temperature range of 25–180  $^{\circ}\text{C}$  and cooled down at a rate of 10  $^{\circ}\text{C}/\text{min}$ .

### 2.4 Field emission scanning electron microscopy (FE-SEM) and EDX testing

The biocomposite specimens' morphology was examined using a field emission scanning electron microscope

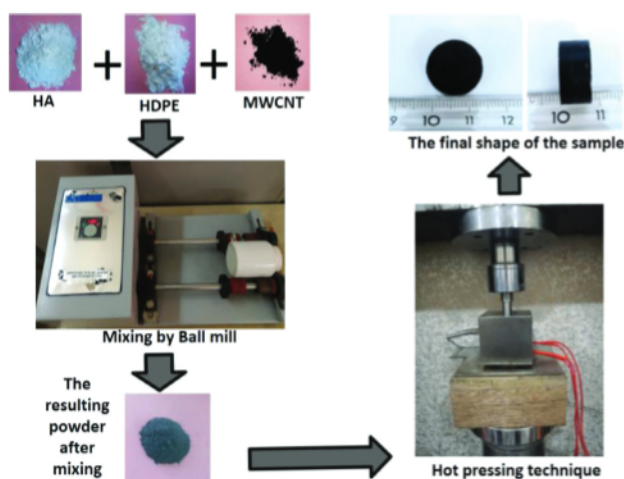


Figure 1: Production of hybrid biocomposite samples

(FE-SEM) (FEI Quanta 450, USA) at an accelerated voltage of 3–10 kV. The samples were coated with a thin layer of gold under vacuum to avoid a heat build-up and electrostatic charging during the examination. An EDX quantitative study was carried out to determine the chemical composition (the Ca/P ratio) of the samples before and after the immersion in Ringer's solution.

### 2.5 X-ray diffraction (XRD)

X-ray powder diffraction is a non-destructive analytical technique and one of the most prospective characterization tools for identifying both inorganic and organic crystalline materials. To determine the crystal structures of the biocomposite samples (HA/HDPE/MWCNT), an XRD analysis was performed using SHIMADZU XRD 6000 whose testing conditions included a voltage of 40 kV, current of 30 mA, drive axis of  $\theta-2\theta$ , scan speed of 10.0000 °/min, sampling pitch of 0.2000° and preset time of 1.20 s.

### 2.6 Immersion in simulated body fluid (SBF)

In this study, a biocompatibility test of the samples was performed in Ringer's solution. Ringer tablets were purchased from Merck Company, Germany. The preparation of the fluid for the biocompatibility test was adopted from the protocol procedure given by the company that provided the tablets. This procedure was performed by dissolving 1 tablet in 0.5 l of distilled water in the autoclave at 121 °C for 15 min. The pieces of equipment used to complete this test are shown in **Figure 2**. The SBF solution temperature was kept at  $37 \pm 0.5$  °C; a hot plate and a thermometer were used. The prepared fluid was replaced every 4 d to maintain the pH value at  $7 \pm 0.5$ . The prepared samples were immersed in Ringer's solution at 37 °C and the bioactivity behavior was assessed with an XRD measurement of each sample after (0, 3, 6, 9, 12) d (after immersing). Also, FE-SEM and EDX were used to complete the assessments.

## 3 RESULTS AND DISCUSSION

### 3.1 AFM results

AFM 3D images recorded the surface topographies of the 40HA/60HDPE samples with different amounts of added MWCNTs as shown in **Figure 3**. The sample microstructures indicate a homogeneous distribution and interconnections between the HA and MWCNT nanoparticles within the HDPE matrix; in addition, the fibrous structure increases with an increased percentage of MWCNTs. **Table 1** lists the differences in the roughness of sample surfaces. The AFM result shows that the maximum surface roughness of 24.023 nm appeared on the sample with a composition of 40HA/60HDPE/2 MWCNT. The roughness of the sample surface has a significant effect on the increase in differentiation and cell proliferation.<sup>15,16</sup> During in vivo investigations, the sur-

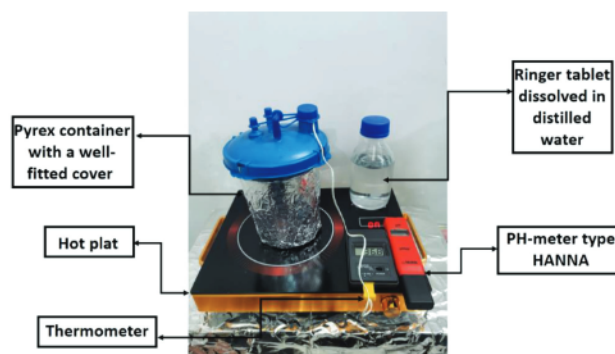


Figure 2: Bioactivity test system

face roughness is one of the most significant parameters for osseointegration. Because of the roughness, the implant topography may simulate the physical signals left by an osteoclast action on the bone surface morphology during the bone-resorption process.<sup>17</sup> Also, researchers explained that an increase in the roughness or surface area of scaffold matrices enhance the osteoblast response, which can lead to an enhanced osteoconductivity of the biomaterial.<sup>18</sup>

Table 1: AFM parameters (peak-peak distance, roughness average and root mean square (RMS) roughness) at different w/% of MWCNTs

Amount of MWCNTs (w/%)	Peak-peak (nm)	Roughness average (nm)	RMS roughness (nm)
0.6	64.664	5.551	7.642
1	170.275	13.93	17.5
1.4	76.28	8.114	10.43
2	207.787	24.023	30.289

### 3.2 DSC result

**Figure 4** shows DSC curves for the 40HA/60HDPE samples, explaining the effect of adding MWCNTs in

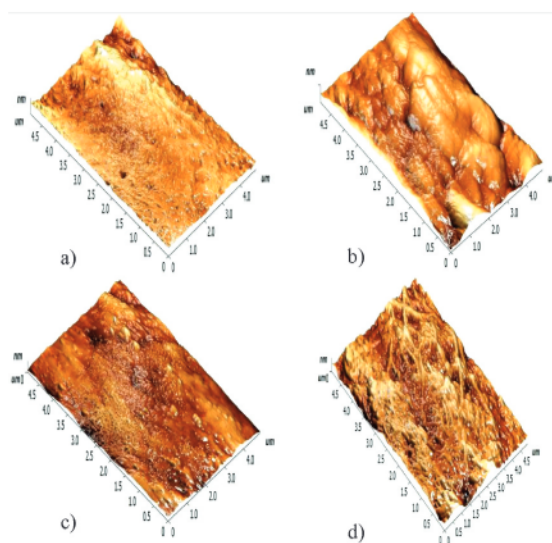


Figure 3: AFM 3D images showing granularity distribution for (40HA/60HDPE): a) 0.6 w/%, b) 1 w/%, c) 1.4 w/%, d) 2 w/% of MWCNTs

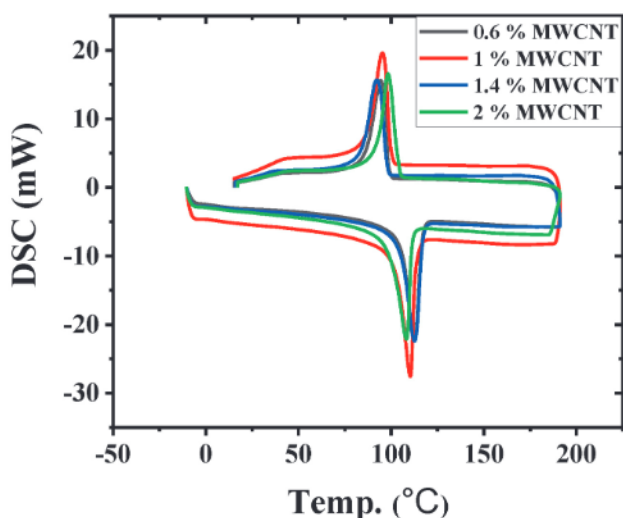


Figure 4: DSC curves for the 40HA/60HDPE composite with various w/% of MWCNTs

different percentages. The area under the melting and crystallization curves of the peak temperature was registered to calculate the melting and crystallization enthalpies ( $\Delta H_m$  and  $\Delta H_c$ ), respectively. The thermal behavior during the heating and cooling of the nanocomposites (HA/HDPE) with various MWCNT w/% is summarized in Table 2. The reasons for decreases in the degree of crystallinity are the entanglement and confinement effects and also the conglomeration of fillers at high HA-additive percentages. Another reason is also the fact that the HA filler has a higher individual heat capacity, which makes it a better heat transmitter, resulting in faster cooling of the composite. This increased cooling rate occurred in the thin lamellar formation, leading to a

lower crystallinity degree.<sup>19</sup> These results show the MWNTs as the nucleating agents, and the previous investigations reported the same.<sup>20,21</sup> On the other hand, when the MWNT addition was increased, the fillers began to block the polymer macromolecular mobilization chains and inhibit macromolecular parts from obtaining a crystal structure.<sup>22</sup> The mechanical properties of polymers increase significantly with an increase in the degree of crystallinity.<sup>23</sup> Thus, it can be proven that the addition of MWCNTs to the composite led to improved mechanical properties.

### 3.3 Bioactivity test

#### 3.3.1 FE-SEM and EDX observations

The FE-SEM analysis was performed before the immersion day, after 6 d and after 12 d of immersion in Ringer’s solution to recognize the HA formation. FE-SEM images of the biocomposite surfaces (40HA/60HDPE) with various w/% of MWCNTs are shown in Figures 5, 6, 7 and 8. It can be observed that the HA layer was deposited on the surfaces of the samples after 6 and 12 d of immersion. Also, we can see that the amount of HA layer developed with the increasing immersion time from 6–12 d; this is in agreement with a previous investigation.<sup>24</sup> The increase in the growth of HA films on the composite surfaces creates the best bioactivity features,<sup>25</sup> supporting osseointegration and bypassing fibrous encapsulation.<sup>26</sup> According to the FE-SEM analysis, the increased MWCNT amount has a significant effect on the structure of the samples, increasing the fibrous structure. The fibrous structure of a sample attracts attention with regard to bone-tissue engineer-

Table 2: Summary of the thermal data based on DSC curves for different w/% of the MWCNT additive to the HA/HDPE/MWCNT biocomposite

Specimen	Melting stage (°C)			$\Delta H_c$ (J/g)	Cooling stage (°C)			$\Delta H_c$ (J/g)	$X_c$ (%)
	( $T_o$ )	( $T_m$ )	( $T_e$ )		( $T_c$ )	( $T_o$ )	( $T_e$ )		
+ 0.6 MWCNT	112.41	105.72	116.65	132.95	94.40	98.72	87.06	122.73	45.8
+1 MWCNT	111.60	104.46	115.88	127.10	94.04	98.86	86.65	119.12	43.8
+1.4 MWCNT	110.60	103.39	114.76	136.86	94.09	99.16	86.70	130.69	47.1
+ 2 MWCNT	112.41	104.55	117.04	162.13	94.00	99.80	86.51	164.96	55.9

$T_m$  – melting peak temperature,  $T_o$  – onset temperature,  $T_e$  – endset temperature,  $\Delta H_m$  – melting enthalpy,  $T_c$  – crystallization peak temperature,  $\Delta H_c$  – crystallization enthalpy,  $X_c$  – degree of crystallinity

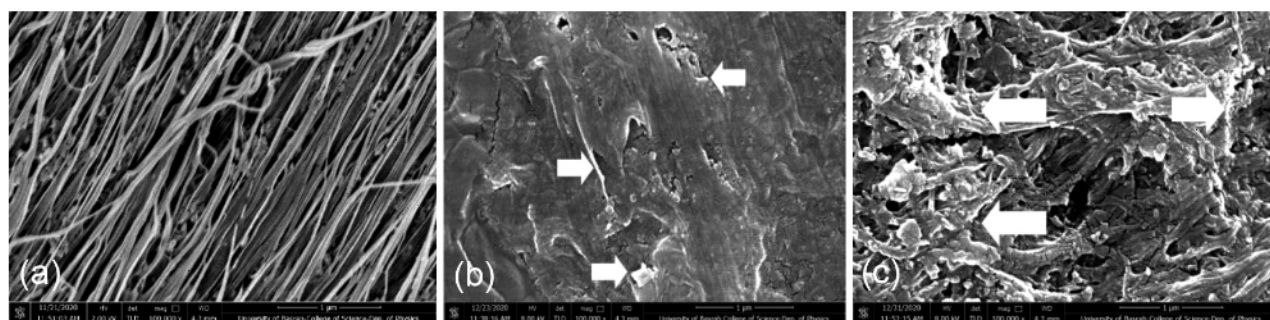


Figure 5: FE-SEM images of the 40HA/60HDPE/0.6 MWCNT composite: a) before 6 d, b) after 6 d, c) after 12 d of immersion in Ringer’s solution (the white arrows indicate the HA layers)

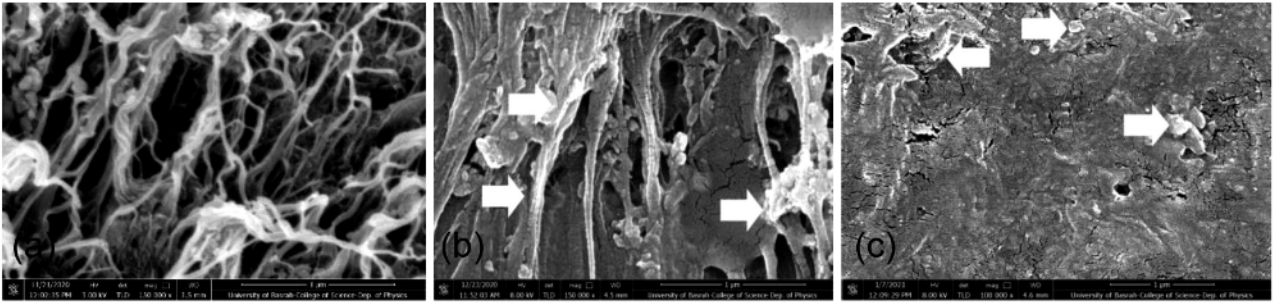


Figure 6: FE-SEM images of the 40HA/60HDPE/1 MWCNT composite: a) before 6 d, b) after 6 d, c) after 12 d of immersion in Ringer's solution (the white arrows indicate the HA layers)

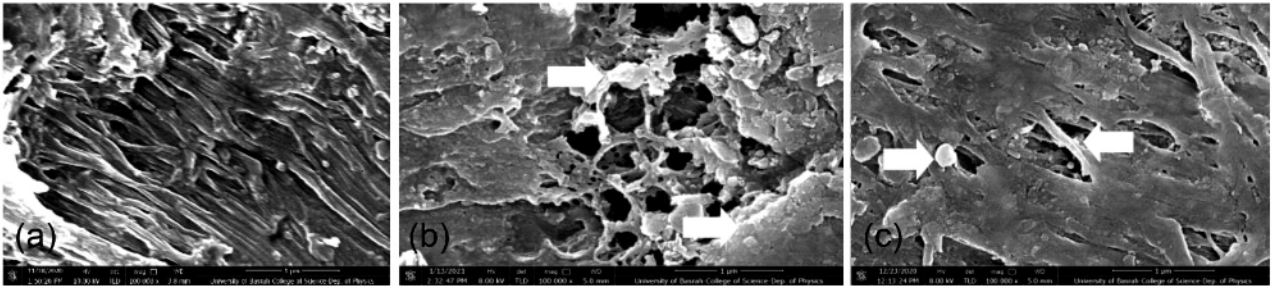


Figure 7: FE-SEM images of the 40HA/60HDPE/1.4 MWCNT composite: a) before 6 d, b) after 6 d, c) after 12 d of immersion in Ringer's solution (the white arrows indicate the HA layers)

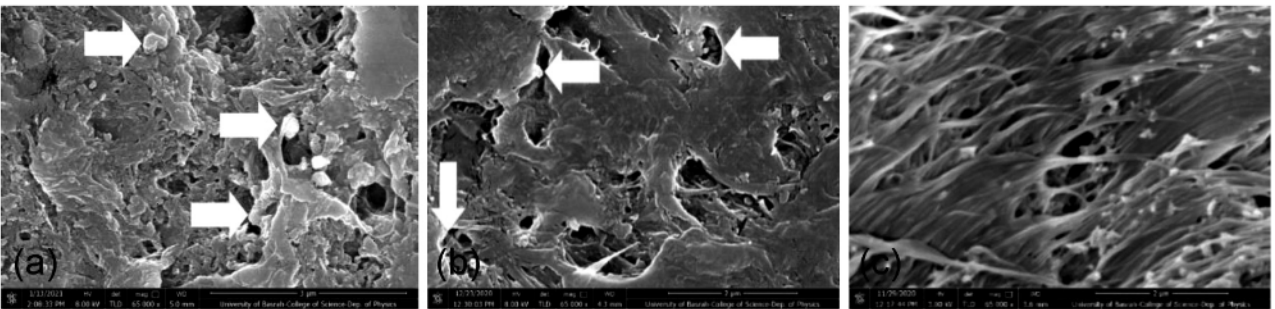


Figure 8: FE-SEM images of the 40HA/60HDPE/2 MWCNT composite: a) before 6 d, b) after 6 d, c) after 12 d of immersion in Ringer's solution (the white arrows indicate the HA layers)

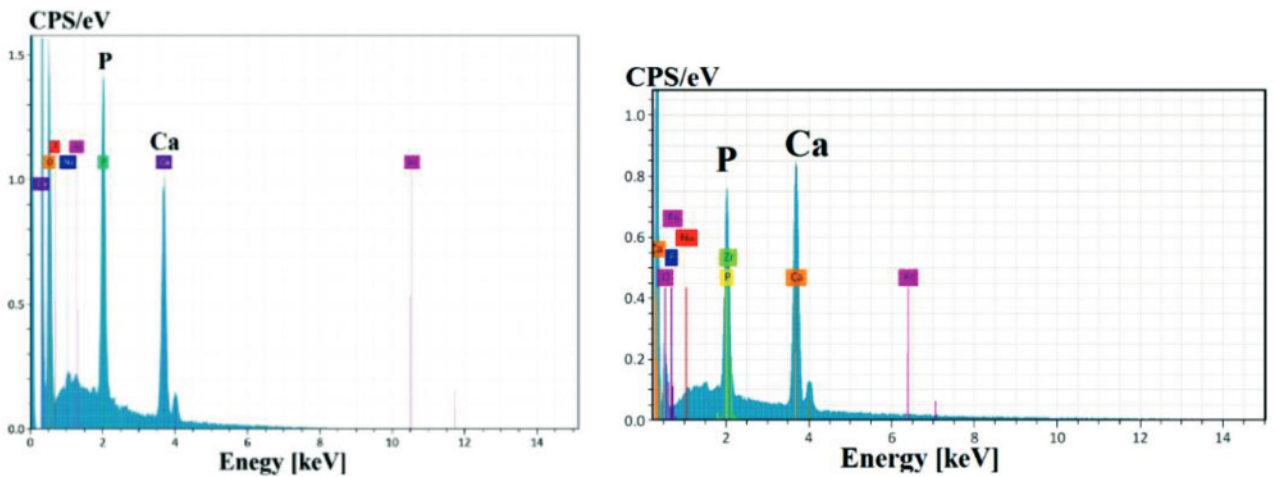


Figure 9: EDX analysis of the 40HA/60HDPE/1 MWCNT sample before and after 12 d of immersion in Ringer's solution

ing not only because it can mimic the natural bone extracellular matrix but also because it can help the tissue to regenerate and integrate it with the neighboring host bone.<sup>27</sup> To better understand a sample's surface bioactivity, the Ca/P ratios were measured and calculated from the EDX spectra, as shown in Figure 9 and Table 3, before and 12 d after the immersion in Ringer's solution. The Ca/P formation appeared on the HA/HDPE composite surface after the immersion in Ringer's solution for 12 d. The result of the bioactivity test agreed with that achieved with FE-SEM. The HA layer covered the composite surface, proving the sample's excellent bioactivity characteristics, which was in agreement with the conclusions reported by other studies.<sup>14,28</sup> Based on the presented results, we recommend the use of the HA/HDPE/MWCNT composite with excellent bioactive characteristics as a substitute material for the bone repair.

**Table 3:** Comparison of the Ca/P ratio obtained during the EDX examination of the spectra of the samples with different w/% of MWCNTs before and after 12 d of immersion in Ringer's solution and Ca/P ratio of natural human bone

MWCNT (w/%)	Ca/P ratio before the immersion day	Ca/P ratio after 12 d of immersion	Ca/P ratio of natural bone
0.6	2.3	4	- 2.31–2.36 for women and men, respectively, in a flat bone <sup>29</sup>
1	2.06	3.17	
1.4	2.41	4.32	- 2.28–2.14 for adults <sup>30,31</sup>
2	2.75	4.2	

### 3.3.2 XRD analysis

The XRD technique is an additional analysis of bioactivity aspects. The XRD results for the 40HA/60HDPE composite before and after the immersion in SBF for (3, 6, 9, 12) d, with various w/% of MWCNTs are shown in Figure 10. It can be observed that the effect of SBF with the immersion time caused a slight shift in  $2\theta$ . This proves the stability of the components of the composites during their exposure to SBF. An in vitro examination of HA such as monetite or brushite is often challenging due to the ion discharge into SBF or adsorption from SBF. These ionic variations are most effective for the cell activity and proliferation.<sup>32</sup> Monetite (dicalcium phosphate anhydrous  $\text{CaHPO}_4$ ) and brushite (dicalcium phosphate dehydrate  $\text{CaHPO}_4 \cdot 2\text{H}_2\text{O}$ ) are other calcium phosphate phases. They can reconstruct bone cells by allowing replacement materials to form a new tissue.<sup>33,34</sup>

Based on the XRD data, an immersion in SBF leads to a change in the crystallographic structure of HA and formation of monetite and brushite. Monetite appeared markedly after 6 d and in the samples that had (0.6, 1.4 and 2) w/% of MWCNTs; in the sample with 1 w/% of MWCNTs, it appeared after 3 d. Brushite exhibits a higher solubility in physiological environments, leading to in vivo bone remodeling due to a more active resorp-

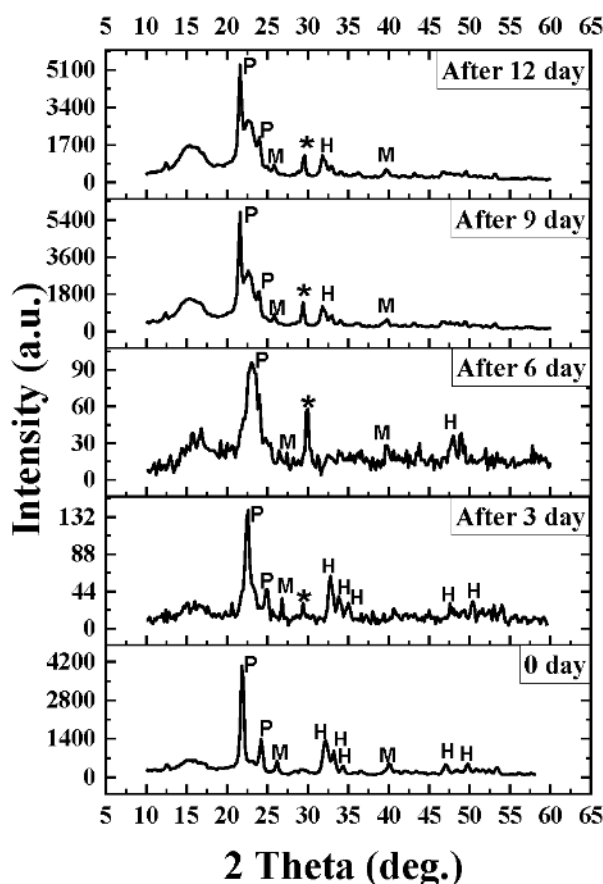


**Figure 10:** XRD patterns of the 40HA/60HDPE composite before and after the immersion in SBF, with 1 w/% MWCNTs (\* denoted monetite, P = HDPE, H = HA, M = MWCNT)

tion. In comparison, monetite exhibits a lower solubility under physiological conditions than brushite, but it is resorbed faster during an in vivo investigation. So, monetite does not convert into HA with a low solubility at the physiological pH. In conclusion, both of them gave promising in vivo results.<sup>32</sup>

## 4 CONCLUSION

The synthesized composites (HA/HDPE) with different w/% of MWCNTs were fabricated using the hot-pressing technique and characterized with several techniques. The surface topography of the samples indicates a homogeneous distribution and interconnections between the components of the composite materials exhibiting fibrous-structure increases with increased amounts of MWCNTs. The maximum roughness of the surface appeared in the sample with 2 w/% of MWCNTs. Hence, the roughness of the sample surface has a significant effect on the differentiation and cell-proliferation increase. Based on a thermal analysis, the percentage of crystallization increased from 45.8 % to 55.9 % when the amount of added MWCNTs increased from 0.6 w/% to 2 w/%. This development in the crystallization degree shows that an excellent enhancement of mechanical properties occurs with an increased percentage of

MWCNTs, as reported in our previous study.<sup>11</sup> The in vitro biological analysis exhibited high bioactivity. The active HA layer formed after the sample immersion in Ringer's solution; this layer also developed with an increase in the immersion time from 6–12 d. The appearance of the HA layer with the fibrous structure of the sample surface allows a better understanding of bioactivity needed for a simulation of natural bone as an extracellular matrix. It can be concluded that the HA/HDPE/MWCNT biocomposite has a great potential to be used as a bone-substitute material.

## Acknowledgements

Thanks to (Dr Imad Ali Disher) from the Faculty of Materials Engineering, University of Babylon, Iraq, for providing exceptional advice during samples fabrication. Extend gratitude to (Eng. Khaldoon Mohammed Khaldoon) for providing support related to administrative matters.

## 5 REFERENCES

- A. A. Nather, Bone grafts and bone substitutes: basic science and clinical applications, World Scientific, (2005), doi:10.1142/5695
- T. Kokubo, H. M. Kim, M. Kawashita, Novel bioactive materials with different mechanical properties, *Biomaterials*, 24 (2003) 13, 2161–2175, doi:10.1016/s0142-9612(03)00044-9
- R. Dimitriou, E. Jones, D. McGonagle, P. V. Giannoudis, Bone regeneration: current concepts and future directions. *BMC Med.*, 9 (2011) 1, 1–10, doi:10.1186/1741-7015-9-66
- R. Z. LeGeros, Properties of osteoconductive biomaterials: calcium phosphates, *Clin. Orthop. Relat. Res.*, 395 (2002), 81–98, doi:10.1097/00003086-200202000-00009
- L. L. Hench, An Introduction to Bioceramics, World scientific, 1 (1993), doi:10.1142/p884
- S. Nath, S. Bodhak, B. Basu, Tribological investigation of novel HDPE-HAp-Al<sub>2</sub>O<sub>3</sub> hybrid biocomposites against steel under dry and simulated body fluid condition, *J. Biomed. Mater. Res. Part A: An Off. J. Soc. Biomater., Japanese Soc. Biomater., Aust. Soc. Biomater., Korean Soc. Biomater.*, 83 (2007) 1, 191–208, doi:10.1002/jbm.a.31203
- K. S. Ibrahim, Carbon nanotubes-properties and applications: a review, *Carbon Lett.*, 14 (2013), 131–144, doi:10.5714/CL.2013.14.3.131
- A. T. Mouad, S. H. Ahmad, Characterization and Morphology of Modified Multi-Walled Carbon Nanotubes Filled Thermoplastic Natural Rubber (TPNR) Composite, In: *Syntheses and Applications of Carbon Nanotubes and Their Composites*, Intech Open, 2013, doi:10.5772/50726
- H. Fouad, R. Elleithy, S. M. Al-Zahrani, M. A. Ali, Characterization and processing of high density polyethylene/carbon nano-composites, *Mater. Des.*, 32 (2011) 4, 1974–1980, doi:10.1016/j.matdes.2010.11.066
- K. Lawton, H. Le, C. Tredwin, R. D. Handy, Carbon Nanotube Reinforced Hydroxyapatite Nanocomposites as Bone Implants: Nanostructure, Mechanical Strength and Biocompatibility, *Int. J. Nanomedicine*, 14 (2019), 7947–7962, doi:10.2147/IJN.S218248
- A. A. Al-allaq, J. S. Kashan, M. T. El-Wakad, A. M. Soliman, Multiwall carbon nanotube reinforced HA/HDPE biocomposite for bone reconstruction, *Periodicals of Engineering and Natural Sciences (PEN)*, 9 (2021) 2, 930–939, doi:10.21533/pen.v9i2.1946
- R. Ma, D. Guo, Evaluating the bioactivity of a hydroxyapatite-incorporated polyetheretherketone biocomposite, *J. Orthop. Surg. Res.*, 14 (2019) 1, 1–13, doi:10.1186/s13018-019-1069-1
- J. Xu, X. Hu, S. Jiang, Y. Wang, R. Parungao, S. Zheng, Y. Nie, T. Liu, K. Song, The Application of Multi-Walled Carbon Nanotubes in Bone Tissue Repair Hybrid Scaffolds and the Effect on Cell Growth In Vitro, *Polymers (Basel)*, 11 (2019) 2, 230, doi:10.3390/polym11020230
- Y. Akgul, H. Ahlatci, M. E. Turan, H. Simsir, M. A. Erden, Y. Sun, A. Kilic, Mechanical, tribological, and biological properties of carbon fiber/hydroxyapatite reinforced hybrid composites, *Polym. Compos.*, (2020), doi:10.1002/pc.25546
- C. Liang, Y. Luo, G. Yang, D. Xia, L. Liu, X. Zhang, H. Wang, Graphene oxide hybridized nHAC/PLGA scaffolds facilitate the proliferation of MC3T3-E1 cells, *Nanoscale Res. Lett.*, 13 (2018) 1, 1–10, doi:10.1186/s11671-018-2432-6
- A. Zareidoost, M. Yousefpour, B. Ghaseme, A. Amanzadeh, The relationship of surface roughness and cell response of chemical surface modification of titanium, *J. Mater. Sci. Mater. Med.*, 23 (2012) 6, 1479–1488, doi:10.1007/s10856-012-4611-9
- A. B. Faia-Torres, S. Guimond-Lischer, M. Rottmar, M. Charnley, T. Goren, K. Maniura-Weber, N. D. Spencer, R. L. Reis, M. Textor, N. M. Neves, Differential regulation of osteogenic differentiation of stem cells on surface roughness gradients, *Biomaterials*, 35 (2014) 33, 9023–9032, doi:10.1016/j.biomaterials.2014.07.015
- A. Yeo, W. J. Wong, H. H. Khoo, S. H. Teoh, Surface modification of PCL-TCP scaffolds improve interfacial mechanical interlock and enhance early bone formation: An in vitro and in vivo characterization, *J. Biomed. Mater. Res. Part A, An Off. J. Soc. Biomater., Japanese Soc. Biomater., Aust. Soc. Biomater., Korean Soc. Biomater.*, 92 (2010) 1, 311–321, doi:10.1002/jbm.a.32366
- O. Y. Allothman, F. N. Almajhdi, H. Fouad, Effect of gamma radiation and accelerated aging on the mechanical and thermal behavior of HDPE/HA nano-composites for bone tissue regeneration, *Biomed. Eng. Online*, 12 (2013) 1, 1–15, doi:10.1186/1475-925X-12-95
- C. Zhu Liao, K. Li, H. Man Wong, W. Yin Tong, K. Wai Kwok Yeung, S. Chin Tjong, Novel polypropylene biocomposites reinforced with carbon nanotubes and hydroxyapatite nanorods for bone replacements, *Mater. Sci. Eng. C*, 33 (2013) 3, 1380–1388, doi:10.1016/j.msec.2012.12.039
- L. Amoroso, E. L. Heeley, S. N. Ramadas, T. McNally, Crystallisation behaviour of composites of HDPE and MWCNTs: The effect of nanotube dispersion, orientation and polymer deformation, *Polymer (Guildf)*, 201 (2020), 122587, doi:10.1016/j.polymer.2020.122587
- A. B. Kaganj, A. M. Rashidi, R. Arasteh, S. Taghipoor, Crystallisation behaviour and morphological characteristics of poly (propylene)/multi-walled carbon nanotube nanocomposites, *J. Exp. Nanosci.*, 4 (2009) 1, 21–34, doi:10.1080/174580802688427
- N. Dusunceli, O. U. Colak, Modelling effects of degree of crystallinity on mechanical behavior of semicrystalline polymers, *Int. J. Plast.*, 24 (2008) 7, 1224–1242, doi:10.1016/j.ijplas.2007.09.003
- H. Balakrishnan, M. R. Husin, M. U. Wahit, M. R. Abdul Kadir, Preparation and characterization of organically modified montmorillonite-filled high density polyethylene/hydroxyapatite nanocomposites for biomedical applications, *Polym. Plast. Technol. Eng.*, 53 (2014) 8, 790–800, doi:10.1080/03602559.2014.886043
- M. R. Husin, M. U. Wahit, M. R. Abdul Kadir, W. A. Wan Abd. Rahman, Effect of hydroxyapatite reinforced high density polyethylene composites on mechanical and bioactivity properties, *Key Engineering Materials*, 471 (2011), 303–308, doi:10.4028/www.scientific.net/KEM.471-472.303
- R. A. Sousa, R. L. Reis, A. M. Cunha, M. J. Bevis, Processing and properties of bone-analogue biodegradable and bioinert polymeric composites, *Compos. Sci. Technol.*, 63 (2003), 3–4, 389–402, doi:10.1016/S0266-3538(02)00213-0
- J. Moy, A. Limaye, T. L. Arinzeh, Fibrous scaffolds for bone tissue engineering, In: *Artif. Protein. Pept. Nanofibers, Des. Fabr. Charact.*

- Appl, online, (2020), 351–382, doi:10.1016/B978-0-08-102850-6.00015-2
- <sup>28</sup> P. K. Chakraborty, J. Adhikari, P. Saha, Variation of the properties of sol-gel synthesized bioactive glass 45S5 in organic and inorganic acid catalysts, *Mater. Adv.*, 2 (2021) 1, 413–425, doi:10.1039/D0MA00628A
- <sup>29</sup> M. Tzaphlidou, V. Zaichick, Calcium, phosphorus, calcium-phosphorus ratio in rib bone of healthy humans, *Biol. Trace Elem. Res.*, 93 (2003) 1, 63–74, doi:10.1385/BTER:93:1-3:63
- <sup>30</sup> A. Salam H. Makhoulf, D. Scharnweber, *Handbook of Nanoceramic and Nanocomposite Coatings and Materials*, Butterworth-Heinemann, 2015, doi:10.1016/C2013-0-13073-5
- <sup>31</sup> S. V. Dorozhkin, M. Epple, Biological and medical significance of calcium phosphates, *Angew. Chemie Int. Ed.*, 41 (2002) 17, 3130–3146, doi:10.1002/1521-3773(20020902)41:17<3130
- <sup>32</sup> M. Schamel, J. E. Barralet, J. Groll, U. Gbureck, In vitro ion adsorption and cytocompatibility of dicalcium phosphate ceramics, *Biomater. Res.*, 21 (2017) 1, 1–8, doi:10.1186/s40824-017-0096-4
- <sup>33</sup> K. Suchanek, A. Bartkowiak, M. Perzanowski, M. Marszałek, From monetite plate to hydroxyapatite nanofibers by monoethanolamine assisted hydrothermal approach, *Sci. Rep.*, 8 (2018) 1, 1–9, doi:10.1038/s41598-018-33936-4
- <sup>34</sup> F. Tamimi, D. Le Nihouannen, H. Eimar, Z. Sheikh, S. Komarova, J. Barralet, The effect of autoclaving on the physical and biological properties of dicalcium phosphate dihydrate bioceramics: Brushite vs. monetite, *Acta Biomater.*, 8 (2012) 8, 3161–3169, doi:10.1016/j.actbio.2012.04.025